remote sensing

MDPI

Article

Estimation of Forest Structural Diversity Using the Spectral and Textural Information Derived from SPOT-5 Satellite Images

Jinghui Meng [1,*,†], Shiming Li [2,*,†], Wei Wang [3], Qingwang Liu [2], Shiqin Xie [1] and Wu Ma [4]

1 Key Laboratory for Silviculture and Conservation of Ministry of Education, Beijing Forestry University, Beijing 100083, China; shiqinxie@126.com
2 Institute of Forest Resource and Information Techniques, Chinese Academy of Forestry, Beijing 100091, China; liuqw@caf.ac.cn
3 Survey & Planning Institute of State Forestry Administration, Beijing 100714, China; didiwei1981@163.com
4 School of Natural Resources, West Virginia University, Morgantown, WV 26506, USA; wuma@mix.wvu.edu
* Correspondence: Jmeng@bjfu.edu.cn (J.M.); lism@caf.ac.cn (S.L.); Tel.: +86-10-6233-8133 (J.M.); +86-10-6288-9804 (S.L.)
† These authors contributed equally to this work.

Academic Editors: Sangram Ganguly, Compton Tucker, Parth Sarathi Roy and Prasad S. Thenkabail
Received: 20 October 2015; Accepted: 25 January 2016; Published: 5 February 2016

Abstract: Uneven-aged forest management has received increasing attention in the past few years. Compared with even-aged plantations, the complex structure of uneven-aged forests complicates the formulation of management strategies. Forest structural diversity is expected to provide considerable significant information for uneven-aged forest management planning. In the present study, we investigated the potential of using SPOT-5 satellite images for extracting forest structural diversity. Forest stand variables were calculated from the field plots, whereas spectral and textural measures were derived from the corresponding satellite images. We firstly employed Pearson's correlation analysis to examine the relationship between the forest stand variables and the image-derived measures. Secondly, we performed all possible subsets multiple linear regression to produce models by including the image-derived measures, which showed significant correlations with the forest stand variables, used as independent variables. The produced models were evaluated with the adjusted coefficient of determination (R^2_{adj}) and the root mean square error (RMSE). Furthermore, a ten-fold cross-validation approach was used to validate the best-fitting models ($R^2_{adj} > 0.5$). The results indicated that basal area, stand volume, the Shannon index, Simpson index, Pielou index, standard deviation of DBHs, diameter differentiation index and species intermingling index could be reliably predicted using the spectral or textural measures extracted from SPOT-5 satellite images.

Keywords: uneven-aged forest management; forest structural diversity; spectral and textural measures; Pearson's correlation analysis; all subsets multiple linear regression

1. Introduction

Forests are the largest territorial ecosystems and play a significant role in providing us with economic benefits as well as ecological services [1,2]. In the past, commodity production was the most significant objective of forest management and forests were mainly managed for producing wood for timber, pulp, and fuel. In recent decades, however, ecological services provided by forests such as soil and water conservation, combating climate change, biodiversity conservation as well as the recreational values of forest landscapes have been highlighted due to the worsening environmental problems [2–4]. In this context, multiple-purpose forest management has been proposed as a silvicultural alternative

to traditional management regimes specialized for even-aged, mono-specific stands [5–8]. Managing forests as complex systems to achieve multiple objectives is receiving increasing attention. [9,10].

System structure determines system function [11]. Likewise, forest functions are determined by forest structure. Forest structure, therefore, is a fundamental base to formulate a sound forest management regime aimed at various objectives. Forest structure can be quantitatively represented by different forest stand variables that vary with respect to detail. For the management of even-aged, mono-specific stands, the conventional forest stand variables such as number of trees (NT), stand volume per unit area (SV), basal area (BA), and quadratic mean diameter (QMD) are considered to be sufficient to prescribe management strategies because such types of forests have a simple structure and are easy to manage. However, these variables fail to describe the complex forest structure of uneven-aged, mixed-species, irregular forests managed for multi-purposes and hence more detailed information should be included. Corona [12] documented that forest inventory and mapping are broadening their scope towards multipurpose resources surveys in the context of global change, utilities from ecosystem management and recent change in forest management perspective.

Forest structural diversity provides a more detailed description of forest stands and is a significant component of forest structure. It can be subdivided into three categories: tree species diversity, tree dimension diversity or tree size diversity, and tree position diversity [13,14]. Forest structural diversity is expected to provide several potential applications as tools for forest management planning. For instance, Lexerod and Eid [15] and O'Hara [16] argued that selective cuttings are most profitable in stands of high tree size diversity whereas clearcuttings should be suggested if the tree size diversity is low. Based on species intermingling, *i.e.*, an index of species diversity, Bettinger and Tang [17] formulated tree-level harvest optimization for structure-based forest management.

The conventional means for the collection of these forest stand variables is via national or regional forest field inventories. For example, in China, there are three types of forest inventories, namely, the national forest inventory (NFI), the forest management planning inventory (FMPI), and the forest operation design operational inventory [18]. In these types of forest inventories, ground plots are installed and forest stand variables are recorded. In the past, the most commonly investigated variables were the conventional forest stand variables as the forest inventory at that time was directly related to timber assessment [19]. However, in the context of multiple-purpose forest management, forest inventories are currently evolving towards multipurpose resource surveys and are broadening their scope in several directions [19–21]. Biodiversity is one of the most popular newly included variables as it is an essential prerequisite to support management decisions to maintain multiple forest ecosystem functions in the long term [19]. Forest inventory by field surveys can indeed provide us with the information about conventional forest stand variables and forest biodiversity for forest management planning as well as forest policy formulation, but they are time consuming, expensive and not spatially exhaustive [22,23]. Furthermore, these inventories are conducted periodically, e.g., five years for NFI and 10 years for FMPI, and therefore up-to-date information cannot be guaranteed.

Remote sensing is widely used as an effective and supportive tool for extracting forest attributes because of its wide scale, rapid data collection and cost savings [1,24]. A large number of studies have been reported with respect to the estimation of forest stand variables or forest mapping using remote sensing data. The most commonly used remote sensing data in forestry include airborne LiDAR data and optical multispectral satellite data, which could be further divided into high spatial resolution satellite data (0.6 m–4 m) and synoptic satellite data of relatively lower resolution [25]. The application of airborne LiDAR and high spatial resolution satellite data are limited due to their high cost as well as small coverage (e.g., swath width of Quickbird, Ikonos, Worldview 1, Worldview 2, and Worldview 3 are 16.8 km, 11.3 km, 17.6 km, 16.4 km, and 13.1 km, respectively), though they are promising in certain applications. For instance, LiDAR was reported to provide promising estimates of forest biomass [26–28], tree height [29–31], and detection of individual tree crowns [32–34]. In comparison, the other optical multispectral satellite data of lower spatial resolution had a relatively large coverage area (e.g., the swath width at the nadir of RapidyEye, SPOT-5, Landsat and MODIS is 77 km, 60 km,

185 km, and 2330 km, respectively), which reduced the cost per unit area. Amongst these optical sensors, Wolter *et al.* [25] argued that SPOT-5 represented a reasonable compromise between high and medium spatial resolution and also had a large coverage area compared with the high spatial resolution of other satellite data.

In the present study, we employed SPOT-5 satellite data as well as field survey data to produce regression models for extracting forest structural information. The objectives can be summarized as follows: (i) determine the correlations between the spectral and textural measures extracted from SPOT-5 imagery and forest stand variables; (ii) develop models predicting forest stand variables with image-derived measures as independent variables; and (iii) produce thematic maps, especially for forest structural diversity, using the produced models.

2. Data and Methods

2.1. Data Source

2.1.1. National Forest Inventory Data

The 8th Chinese National Forest Inventory (CNFI) data of Guangxi Zhuang Autonomous Region, collected in 2015, were used. The inventory consists of a systematic sample of permanent square plots with a size of 1 Mu (Chinese unit of area, 0.067 ha) distributed on a square grid of 4 km × 6 km (Figure 1). In each plot, all trees were identified to the species level and their diameter (dbh) as well as their spatial location were recorded.

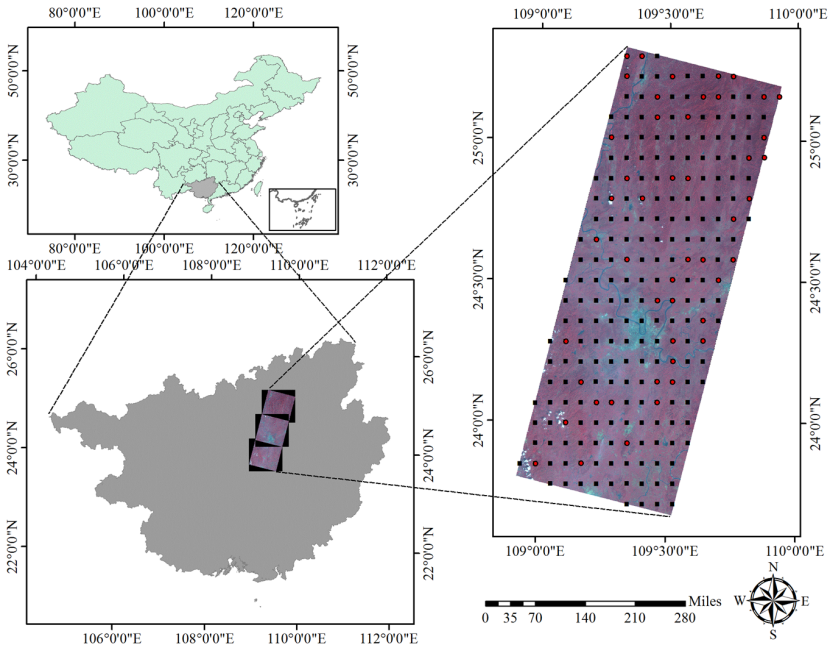

Figure 1. Overview and zoomed map of the study area. The zoomed maps consist of three SPOT-5 image footprints in which the red circle represents the forest plots.

2.1.2. Remote Sensing Data

Three SPOT-5 images, which had the K-J numbers 275/300, 275/301, and 275/302, taken on 21 September 2010, were used in the present study (Figure 1). The three SPOT-5 images consisted of both multi-spectral and panchromatic images. The multi-spectral images have a resolution of 10 m in the near-infrared (780–890 nm), red (610–680 nm) and green (500–590 nm) bands and 20 m in the shortwave infrared (1580–1750 nm) band. The panchromatic image was recorded at a resolution of 2.5 m.

Geometrical corrections were performed using Ground Control Points (GCP), determined with a differential GPS. Atmospheric correction was carried out using the improved Dark Object Subtraction suggested by Castillo-santiago *et al.* [35]. The processing of these images was performed by the Survey & Planning Institute of State Forestry Administration, China prior to the present study. A total of 233 NFI plots fell into these three satellite images, of which 65 plots were dominated by trees. Amongst these 65 plots, there were 48 plots with canopy cover more than 20%, which were defined as forest stands (Figure 1). These 48 plots were employed to derive forest stand variables.

2.2. Forest Stand Variables (Dependent Variables)

2.2.1. Conventional Forest Variables

The conventional forest variables, including quadratic mean diameter (QMD), basal area (BA), number of trees (NT), and stand volume (SV), were calculated for each plot. These variables provide a basic description of forest structure and were mostly derived information for forest management decision-making purposes.

2.2.2. Forest Structural Diversity

In comparison to conventional forest variables, forest structural diversity provides more details on forest structure [15]. Structural diversity can be subdivided into three categories: tree species diversity, tree dimension diversity, and tree position diversity [13,14].

Species Diversity

We used the Shannon–Wiener index (SHI), Pielou index (PI), Simpson's index (SII) and the species intermingling index to characterize species diversity [36].

Shannon–Wiener index:

$$\mathrm{SHI} = -\sum_{i=1}^{n} p_i \cdot \ln\left(p_i\right) \tag{1}$$

where p_i is the proportion of basal areas in the ith species.

Pielou index:

$$\mathrm{PI} = \frac{SHI}{ln(S)} \tag{2}$$

where SHI is the Shannon–Wiener index and S is the total number of species in a sample, across all samples in a dataset.

Simpson's index:

$$\mathrm{SII} = 1 - \sum_{i=1}^{n} p_i^2 \tag{3}$$

where *pi* is the proportion of basal areas in the *i*th species and n is the number of species observed.

The species intermingling index of a forest stand ($\overline{M}$):

$$\overline{M} = \frac{1}{n}\sum_{i=1}^{n} M_i = \frac{1}{4n}\sum_{i=1}^{n}\sum_{j=1}^{4} v_{ij} \tag{4}$$

where $v_{ij} = \begin{cases} 0, if\ neighbour\ j\ is\ the\ same\ species\ as\ reference\ tree\ i \\ 1,\ otherwise \end{cases}$; *Mi* is the species intermingling index for reference tree *i*.

$\overline{M}$ ranges from zero to one and indicates the degree of mixing in a forest stand. Values close to zero indicate that the forest stand has a low level of species mingling and a high degree of aggregation. High values that are close to one, on the other hand, imply that the forest stand has a high level of species mingling and a low degree of aggregation [37].

Diameter or Tree Size Diversity

Tree size diversity can be measured by the Gini coefficient (GC) and the standard deviation of the DBHs (SDDBH) [13,15].

Gini coefficient:

$$GC = \frac{\sum_{t=1}^{n}(2t - n - 1)ba_t}{\sum_{t=1}^{n} ba_t(n-1)} \quad (5)$$

where ba_t is basal area for tree in rank t (m^2/ha) and t is the rank of a tree in order from 1, . . . , n.

GC ranged from zero to one. The GC has a minimum value of zero, when all trees are of equal size, and a theoretical maximum of one in an infinite population in which all trees except one have a value of zero for basal area.

Tree Position Diversity

Tree position diversity can be represented by the uniform angle index, DBH dominance index and Diameter differentiation index [37–39]. These indices have been widely employed in analyzing spatial structure and thus support the formulation of management strategy especially for mixed, irregular, uneven-aged forests [17,40].

Uniform angle index of a forest stand ($\overline{W}$):

$$\overline{W} = \frac{1}{n}\sum_{i=1}^{n} W_i = \frac{1}{4n}\sum_{i=1}^{n}\sum_{j=1}^{4} z_{ij} \quad (6)$$

where $z_{ij} = \begin{cases} 1, \ if \ the \ jth \ \alpha < \alpha_0 \\ 0, \ if \ the \ jth \ \alpha > \alpha_0 \end{cases}$ ($\alpha_0 = 72^\circ$); n is the number of reference trees in the forest stand; i is any reference tree; j is the four nearest trees around reference tree i; and Wi is the uniform angle index, describing the uniformity of the distribution of neighboring trees around the reference tree i.

If $\overline{W}$ falls within [0.475, 0.517], it represents a random distribution; $\overline{W} > 0.517$ represents a clumpy distribution, and $\overline{W} < 0.475$ represents a uniform distribution [41].

The DBH dominance index of a forest stand ($\overline{U}$):

$$\overline{U} = \frac{1}{n}\sum_{i=1}^{n} U_i = \frac{1}{4n}\sum_{i=1}^{n}\sum_{j=1}^{4} k_{ij} \quad (7)$$

where $k_{ij} = \begin{cases} 0, if \ neighbour \ j \ is \ smaller \ than \ reference \ tree \ i \\ 1, \ otherwise \end{cases}$; Ui is the DBH dominance index for reference tree i.

$\overline{U}$ explains the tree size differentiation within a forest stand; its value fall between 0 and 1. The higher the value, the greater the tree size differentiation in the forest stand [37].

Diameter differentiation index (DDI):

The diameter differentiation T_i quantifies diameter heterogeneity in the immediate neighborhood of a tree i. For a central tree i (I = 1, . . . , n) and its nearest neighbors j (j = 1, . . . , m), the diameter differentiation Ti is defined as:

$$T_i = \frac{1}{m}\sum_{j=1}^{m} T_{ij} \quad (8)$$

with

$$T_{ij} = 1 - \frac{\min(DBH_i, DBH_j)}{\max(DBH_i, DBH_j)} \quad (9)$$

where n is the number of central trees, m is the number of neighor trees (m = 3 in present study) and DBH_i and DBH_j are the diameter of the central tree and its neighbors, respectively.

In the present study, we calculated the mean DDI ($\overline{T}$) within a stand using the following equation:

$$\overline{T} = \frac{1}{n}\sum_{i=1}^{n} T_i \tag{10}$$

The above tree position diversity indices could be significantly influenced by the edge trees since some of their neighbor trees might fall outside the plot [42]. It is therefore necessary to conduct edge correction. In this study we used the reflection method.

2.3. Imagery-Derived Measures (Independent Variables)

2.3.1. Spectral Measures

We derived spectral measures from both panchromatic and multispectral reflectance bands. The following spectral measures were calculated for each plot as the potential predictor variables: (1) the average surface reflectance of all pixels inside the field-plot of the spectral bands (mean_green, mean_red, mean_mir and mean_nir) and PANchromatic band (mean_pan); (2) Two-layer value features, *i.e.*, Brightness and Max_Diff. [43]; and (3) Eight vegetation indices, *i.e.*, Normalized Difference Vegetation Index (NDVI) [44], Simple Ratio (SR) [45], Ratio of NIR to GREEN (GR) [46], Ratio of GREEN to RED (VI) [47], Soil Adjusted Vegetation Index (SAVI) [48], Global Environment Monitoring Index GEMI [49], Moisture Stress Index (MSI) [25], and Standardized Vegetation Index (SVR) [25], which are commonly used in forestry research and calculated as shown in Equations (10)–(17).

$$\text{NDVI} = \frac{NIR - RED}{NIR + RED} \tag{11}$$

$$\text{SR} = \frac{NIR}{RED} \tag{12}$$

$$\text{GR} = \frac{NIR}{GREEN} \tag{13}$$

$$\text{VI} = \frac{GREEN}{RED} \tag{14}$$

$$\text{SAVI} = \frac{NIR - RED}{NIR + RED + L} \tag{15}$$

$$\text{SAVI} = \frac{NIR - RED}{NIR + RED + L} \tag{16}$$

$$\text{MSI} = \frac{SWIR}{NIR} \tag{17}$$

$$\text{SVR} = \frac{SWIR}{(\frac{RED + GREEN}{2})} \tag{18}$$

where RED, GREEN, NIR, and SWIR are the surface reflectance of the red, green, near-infrared and shortwave infrared bands, respectively, and L was set to 0.5; and

$$\eta = \frac{2(NIR^2 - RED^2) + 1.5NIR + 0.5RED}{NIR + RED + 0.5} \tag{19}$$

2.3.2. Textural Measures

First- and second-order textural measures were derived for each plot. The first-order textural feature (standard deviation of gray levels, SDGL) was calculated for all multispectral reflectance bands, producing SDGL_green, SDGL_red, SDGL_nir and SDGL_mir.

The panchromatic band is reported to be particularly well suited for the analysis of spatial relationships using image textural measures [22,50–52]. As a result, we only extracted the second-order textural measures from the panchromatic band for each plot in comparison to the spectral and first-order textural measures.

The second-order textural feature was calculated based on the grey level co-occurrence matrix (GLCM). Eight GLCMs—Mean, Std. Dev., Correlation, Dissimilarity, Entropy, angular second moment (ASM), Contrast and Homogeneity—were selected for this study as the potential independent variables to establish the predictive models. A more detailed description of these textural measures is provided by Trimble [43]. In addition to the spatial resolution, the value of the textural variables depends on window size. To determine the optimum window size, Shaban and Dikshit [53] and Castillo-santiago *et al.* [35] calculated and compared the Pearson correlation coefficient of texture statistics with the dependent variables (forest stand variables) at different window sizes and concluded that a 9×9 pixel window represented a trade-off between a desirable high correlation coefficient and a desirable minimum window size. Following them, we calculated the Pearson correlation coefficient of texture statistics with SHI and DDI, at seven window sizes (3×3, 5×5, 7×7, 9×9, 11×11, 13×13 and 15×15 pixels).

2.4. Model Construction and Validation

Prior to producing the predictive models, pairwise correlation analysis was first conducted between the forest stand variables and the image-derived measures. A two-tailed *t*-test was used to determine whether the correlations were statistically significant. Only the image-derived variables that showed significant correlations with the forest stand variables were included as independent variables for the subsequent multiple-variable regression. In order to correct nonlinearity and non-constant variance, we used Box-Cox transformations of the response variables (forest stand variables). For the determination of the potential subset of independent variables, there are two distinctly different approaches, namely, all possible subsets and stepwise methods [54]. In the present study, we used all possible subsets. Following Castillo-Santiago *et al.* [35], Ozdemir and Karnieli [13] and Wallner *et al.* [55], we employed a cut-off value for variance inflation factor (VIF) of less than four, and restricted the number of independent variables to four to avoid multicollinearity.

The general fitting statistics including the adjusted coefficient of determination (R^2_{adj}), and the root mean square error (RMSE) between observed and predicted forest stand variables was computed to evaluate the overall accuracy of the fitted models. In addition, residual plots were produced to inspect the normal distribution of the residuals. For model validation, a ten-fold cross-validation approach was employed to calculate the cross-validated root mean square error ($RMSE_{cv}$). In this approach, all candidate plots for constructing the predictive models were divided into ten folds. In each iteration, one fold was excluded and the remaining folds were retained for regression. The produced models were used to provide predictions pertaining to the excluded fold. The residuals were calculated for each data point in the excluded data and the corresponding $RMSE_i$ was derived. This process was carried out for all folds and the $RMSE_{cv}$ was calculated as the mean of all the $RMSE_i$.

3. Results

3.1. Structural Parameters

The descriptive forest stand variables derived from the 48 sampling plots are summarized in Table 1. Although the number of sampling plots is only 48, they represent a wide range of forest structural characteristics. For instance, SV, one of the most important conventional forest stand variables, ranged from 21.02 m^3/ha to 263.13 m^3/ha with a mean value of 101.23 m^3/ha, which is almost the same as the average value of 100.20 m^3/ha in Guangxi Zhuang Autonomous Region [56]. In terms of species diversity, SHI, for example, ranged from 0 to 1.801, which indicates that the sampling plots contained both single-tree species and mixed-tree species stands, representing a wide range of species diversity. GC ranged from 0.062 to 0.362 with an average value of 0.230, implying a relatively low degree of tree

size diversity because the theoretical maximum value is 1. With respect to tree position diversity, the range of $\overline{M}$ from 0 to 0.778 indicated that the stands varied considerably in species intermingling from a very low level to an extremely high level. $\overline{U}$ ranged from 0.470 to 0.531 with an average value of 0.482, implying that in the stands, tree size was moderately differentiated. $\overline{W}$ ranged from 0.273 to 0.706 with an average value of 0.498. Eight plots were uniform distribution ($\overline{W} < 0.475$), 16 plots were clumpy distribution ($\overline{W} > 0.517$) and 24 plots fell within [0.475, 0.517], representing random distribution.

Table 1. Descriptive statistics of the conventional forest parameters and structural diversity indices of the 48 plots.

Parameters	Mean	S.D	Min.	Max.
Quadratic mean diameter (QMD) (cm)	13.10	3.10	6.58	21.75
Basal area (BA) (m^2/ha)	18.36	10.04	4.41	40.44
Number of trees (NT) (n/ha)	1579	923	254	4313
Stand volume (SV) (m^3/ha)	101.23	57.80	21.02	263.13
Shannon–Wiener index (SHI)	0.920	0.510	0	1.801
Pielou index (PI)	0.263	0.162	0	0.497
Simpson's index (SII)	0.495	0.245	0	0.803
Gini coefficient (GC)	0.230	0.072	0.062	0.362
Standard deviation of DBHs (SDDBH)	4.913	2.227	0.951	11.197
Uniform angle index ($\overline{W}$)	0.498	0.09	0.273	0.706
Species intermingling index ($\overline{M}$)	0.398	0.279	0	0.778
DBH dominance index ($\overline{U}$)	0.482	0.023	0.470	0.531
Diameter differentiation index (DDI)	0.259	0.094	0.096	0.429

3.2. Correlation Analyses

The correlation analyses between the forest stand variables and spectral measures are summarized in Table 2. The average surface reflectance of all bands was significantly negatively correlated with the forest stand variables except $\overline{W}$ and $\overline{U}$. Specifically, the average surface reflectance of the nir, red, green and pan bands showed much higher correlation ($|r| > 0.60$) with SHI, SII, PI and $\overline{M}$. The vegetation indices except GEMI, MSI, SVR were significantly correlated with some forest stand variables, amongst which VI and SAVI were correlated with almost all stand variables and showed a much higher correlation ($|r| > 0.60$) with SHI, SII, PI and $\overline{M}$. Regarding the layer value features, Brightness was significantly correlated with all forest stand variables expect $\overline{W}$ and $\overline{U}$ and the correlation was extremely high with SHI, SII, PI and $\overline{M}$($|r| > 0.70$). Max_diff was only correlated with QMD, BA, NT, SDDBH and SV.

The Pearson correlation coefficient between correlation (a texture statistics) and SHI increased until a window size of 9 × 9 pixels was reached and no further significant improvement was observed when continuing increasing the window up to 15 × 15 pixels (Figure 2). In comparison, the Pearson correlation coefficient between the other texture statistics did not show any notable change along with the window size. Similar pattern was also observed for DDI (Figure 2). The window size of 9 × 9 pixels was therefore determined to be the optimum size to calculate the texture statistics, which was consistent with the findings reported by Shaban and Dikshit [53] and Castillo-santiago *et al.* [35].

In terms of the relationship between textural measures and forest stand variables, the first-order textural measures did not show significant correlation with many forest stand variables, except SDGL_red. For instance, SDGL_swir and SDGL_green were significantly correlated with only two stand variables and the correlations were also not high ($|r| < 0.4$). In contrast, the second-order textural measures exhibited significant correlation with much more forest stand variables. For example, Glcm_contrast, Glcm_mean and Glcm_variance, were highly correlated with all the forest stand variables except $\overline{W}$ and $\overline{U}$. Similarly, much higher correlations were observed between these textural measures and SHI, SII, PI and $\overline{M}$. For example, the correlation coefficient between Glcm_mean and SHI was −0.812, which was ranked as the highest value in the present study.

Table 2. Pearson correlation coefficients between the spectral image measures and the forest stand variables.

Variables	Mean_nir	Mean_red	Mean_green	Mean_swir	Mean_pan	Brightness	Max_diff	NDVI	SR	VI	GEMI	GR	MSI	SAVI	SVR
NT	−3.712 *	−3.870 *	−0.312	−2.998	−0.401 **	−0.472 *	0.397 *	0.301	0.242	0.356 *	−0.098	0.214	0.036	−0.323 *	0.059
QMD	−0.413 *	−0.432 *	−0.461 *	−3.242 *	−0.422 *	−0.488 *	0.444 *	0.298	0.274	0.410 *	−0.214	0.256 *	0.056	−0.419 *	0.023
BA	−0.522 **	−0.554 **	−0.543 **	−0.436 **	−0.533 **	−0.598 **	0.561 **	0.329 *	0.314	0.507 **	−0.318 *	0.315	0.016	−0.511 **	0.099
SV	−0.512 **	−0.580 **	−0.536 **	−0.450 *	−0.526 **	−0.601 **	0.555 **	0.346 *	0.312	0.512 **	−0.307	0.299	0.012	−0.493 *	0.111
GC	−0.401 *	−0.524 **	−0.479 *	−0.384 *	−0.467 *	−0.454 *	0.101	0.379 *	0.383 *	0.454 *	−0.270	0.221	0.018	−0.424 *	0.276
DDI	−0.458 *	−0.522 **	−0.486 **	−0.352 *	−0.520 **	−0.515 **	0.044	0.257	0.260	0.594 **	−0.141	0.078	0.008	−0.457 *	0.115
SDDBH	−0.491 *	−0.546 **	−0.520 **	−0.478 *	−0.546 **	−0.557 **	0.341 *	0.274	0.291	0.602 **	−0.146	0.074	−0.166	−0.490 *	0.023
SHI	−0.646 **	−0.829 **	−0.824 **	−0.492 *	−0.808 **	−0.786 **	0.078	0.532 **	0.538 **	0.824 **	−0.260	0.305	0.054	−0.645 **	0.353 *
SII	−0.589 **	−0.775 **	−0.768 **	−0.467 *	−0.761 **	−0.733 **	0.072	0.502 **	0.504 **	0.766 **	−0.303	0.286	0.004	−0.588 **	0.284
PI	−0.632 **	−0.798 **	−0.782 **	−0.494 *	−0.771 **	−0.763 **	0.110	0.484 *	0.488 *	0.817 **	−0.300	0.248	0.008	−0.631 **	0.276
$\overline{M}$	−0.629 **	−0.781 **	−0.759 **	−0.541 **	−0.757 **	−0.777 **	0.123	0.434 *	0.436 *	0.831 **	−0.114	0.197	−0.104	−0.628 **	0.141
$\overline{U}$	−0.003	−0.115	−0.098	−0.114	−0.109	−0.095	0.100	0.147	0.155	0.145	−0.045	0.128	−0.189	−0.002	−0.030
$\overline{W}$	−0.100	−0.129	−0.123	0.0142	−0.131	−0.094	−0.160	0.109	0.109	0.166	−0.068	0.060	0.1402	−0.010	0.152

* Correlation is significant at the 0.05 level (2-tailed); ** Correlation is significant at the 0.01 level (2-tailed).

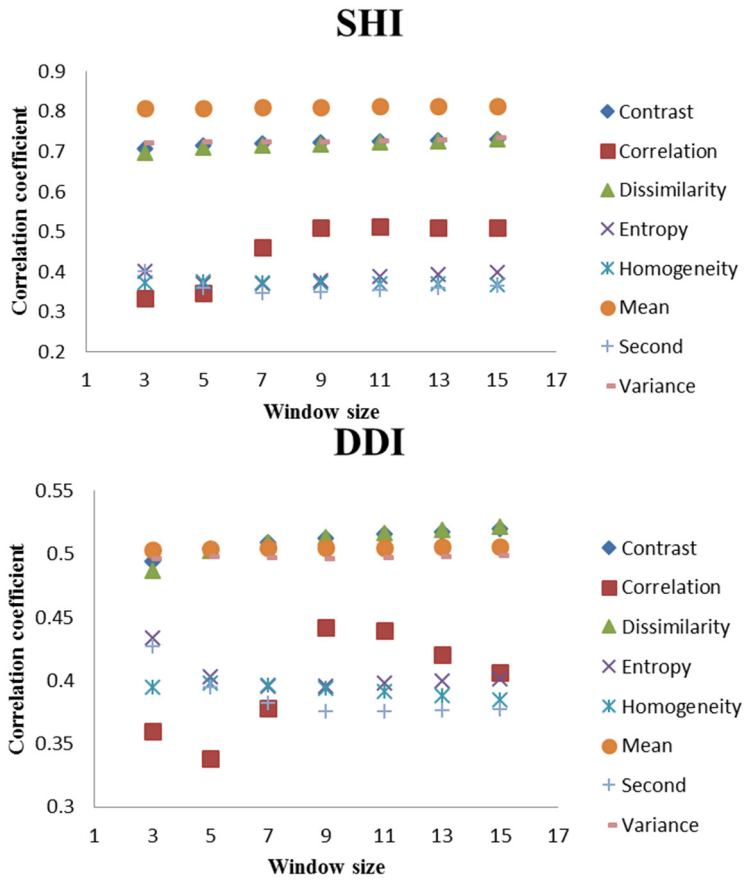

Figure 2. Correlation coefficient of the texture statistics with SHI and DDI, as a function of window size.

3.3. Model Establishment

We first produced the predictive models using both textural and spectral measures as independent variables. Although most of the textural measures and the spectral measures indicated a significant correlation with the forest stand variables (Tables 2 and 3), we excluded some of them to avoid multicollinearity. The produced models are summarized in Table 4. The developed models had at most three independent variables. Brightness was the most commonly used independent variable in the models predicting BA, QMD, SV, NT and SDDBH. The following one was Max_diff, which contributed to the models predicting BA, QMD, SV and NT. VI and mean_red ranked third. VI was an independent variable in the models predicting PI, $\overline{M}$ and DDI, whereas mean_red was involved in the models predicting SHI, SII, and GC. The other independent variables for the models included SDGL_nir, SDGL_green and SDGL_nir.

All regression models were statistically significant ($p < 0.01$), but we concluded that the models (1, 3, 4, 5, 8, 9, 10, 11 and 12) predicting BA, SV, SHI, SII, SDDBH, PI, DDI and $\overline{M}$ were reliable as their adjusted correlation coefficients (R^2_{adj}) were equal to or greater than 0.5. The RMSEs for the precedent models (1, 3, 4, 5, 8, 9, 10, 11 and 12) were 0.856, 2.217, 0.308, 0.182, 0.125, 0.136, 0.067, 0.149, and 0.128, respectively (Table 4). The prediction abilities of these models were further substantiated by the cross-validation scores calculated from the ten-fold cross-validation approach ($RMSE_{cv}$ values were 0.872, 2.303, 0.326, 0.195, 0.132, 0.148, 0.072, 0.158, and 0.133).

Table 3. Pearson correlation coefficients between the textural image measures and the forest structural parameters.

Variables	SDGL _nir	SDGL _red	SDGL _green	SDGL _swir	SDGL _pan	Glcm _ASM	Glcm _contrast	Glcm _correlation	Glcm _dissimilarity	Glcm _entropy	Glcm _homogeneity	Glcm _mean	Glcm _variance
NT	0.245	−0.156	0.124	0.270	−0.152	0.110	−0.391 *	0.186	−0.377 *	−0.147	0.196	−0.482 *	−0.419 *
QMD	0.315	−0.315	0.169	0.319 *	−0.136	0.139	−0.420 *	0.095	−0.419 *	−0.125	0.266	−0.491 *	−0.466 *
BA	0.266	−0.245	0.312	0.153	−0.214	0.259	−0.493 *	0.149	−0.507 **	−0.247	0.292	−0.534 **	−0.501 **
SV	0.275	−0.296	0.302	0.125	−0.256	0.275	−0.504 **	0.172	−0.524 **	−0.270	0.280	−0.559 **	−0.521 **
GC	0.396 *	−0.268	−0.189	0.290	−0.310	0.213	−0.446 *	0.320 *	−0.510 **	−0.197	0.211	−0.525 **	−0.497 *
DDI	0.466 *	−0.398 *	−0.397 *	0.313	−0.362 *	0.376 *	−0.513 **	0.442 *	−0.513 **	−0.400 *	0.460 *	−0.505 **	−0.497 *
SDDBH	0.456 *	−0.426 *	−0.208	0.336 *	−0.328 *	0.209	−0.535 **	0.362 *	−0.532 **	−0.232	0.254	−0.542 **	−0.513 **
SHI	0.250	−0.362 *	−0.262	0.064	−0.208	0.349 *	−0.722 **	0.511 **	−0.719 **	−0.379 *	0.392 *	−0.812 **	−0.726 **
SII	0.231	−0.381 *	−0.316 *	0.035	−0.240	0.368 *	−0.690 **	0.496 *	−0.698 **	−0.393 *	0.378 *	−0.764 **	−0.697 **
PI	0.261	−0.408 *	−0.306	0.091	−0.228	0.383 *	−0.694 **	0.491 *	−0.709 **	−0.426 *	0.412 *	−0.776 **	−0.697 **
$\overline{M}$	0.284	−0.456 *	−0.385 *	0.066	−0.270	0.397 *	−0.676 **	0.534 **	−0.704 **	−0.421 *	0.382 *	−0.759 **	−0.676 **
$\overline{U}$	0.261	−0.060	−0.098	0.208	0.004	0.136	−0.118	−0.032	−0.138	−0.129	0.151	−0.111	−0.116
$\overline{W}$	0.138	−0.112	−0.123	0.181	−0.146	0.013	−0.102	0.250	−0.1152	−0.058	0.057	−0.130	−0.109

* Correlation is significant at the 0.05 level (2-tailed); ** Correlation is significant at the 0.01 level (2-tailed).

Table 4. Regression model predicting the forest stand variables using both spectral and textural measures as independent variables.

Forest Stand Variables	Predictive Model	R^2_{adj}	RMSE	*p*
Basal area (BA)	Model 1: BA ^0.4 = −0.023894· Brightness + 2.416160· Max_diff + 4.281999	0.52	0.856	9.837×10^{-8}
Quadratic mean diameter (QMD)	Model 2: QMD^(−0.3) = 0.0010350· Brightness − 0.1741902· Max_diff + 0.4416836	0.32	0.033	4.856×10^{-5}
Stand volume (SV)	Model 3: SV^0.3 = 3.59910 − 0.0157· Brightness +3.45959· Max_diff	0.50	2.217	3.154×10^{-7}
Shannon–Wiener index (SHI)	Model 4: SHI^0.7 = −0.026641· mean_red + 3.060631	0.62	0.309	2.854×10^{-8}
Simpson's index (SII)	Model 5: SII^1.1 = −0.01513· mean_red + 1.70493	0.60	0.182	8.735×10^{-8}
Gini coefficient (GC)	Model 6: GC = 0.334589 − 0.001584· mean_red	0.42	0.046	4.643×10^{-6}
Number of trees (NT)	Model 7: NT^0.6 = 107.9658 − 0.4471· Brightness + 14.0616· Max_diff	0.21	21.322	4.789×10^{-6}
Standard deviation of DBHs (SDDBH)	Model 8: SDDBH^0.2 = −0.007714· Brightness + 0.021443· SDGL_nir + 1.929803	0.51	0.125	2.849×10^{-6}
Pielou index (PI)	Model 9: PI^0.6 = 3.2225· VI − 4.1580	0.60	0.136	6.676×10^{-8}
Diameter differentiation index (DDI)	Model 10: DDI^0.7 = 0.8917· VI − 0.0118· SDGL_nir − 0.0382· SDGL_green − 0.8697	0.57	0.067	4.17×10^{-6}
Species intermingling index ($\overline{M}$)	Model 11: $\overline{M}$^0.9 = 4.5530· VI − 5.9967	0.68	0.149	2.697×10^{-9}
Species intermingling index ($\overline{M}$)	Model 12: $\overline{M}^*$^0.9 = −4.8341 + 3.7593· VI	0.70	0.128	3.942×10^{-6}

* Species intermingling index calculated from all the plots excluding the plots of pure plantation.

The residual plots of the reliable models are presented in Figure 3, and no particular patterns were observed. We therefore concluded that these models had potential to predict and map the forest stand variables. Based on model 5, the thematic map of Simpson's index was produced as an example (Figure 4).

As many studies have demonstrated that forest stand variables can be estimated using only textural measures as independent variables, for comparison purposes, the predictive models were also built using only textural measures as independent variables. All of the produced models except the ones predicting $\overline{M}$ and DDI, had only one independent variable, which was Glcm_mean. Amongst all the twelve models in Table 5, only models (15, 16, 20, 22 and 23) predicing SHI, SII, PI and $\overline{M}$ could be trusted as their adjusted correlation coefficients (R^2_{adj}) were larger than 0.5. Their RMSEs were 0.321, 0.170, 0.127 and 0.160 and 0.147, respectively (Table 5). The residuals of the models were normally distributed and showed evidence of uniform variance (Figure 5). Their prediction abilities were substantiated by the cross-validation scores ($RMSE_{cv}$ values were 0.342, 0.174, 0.134, 0.166 and 0.155).

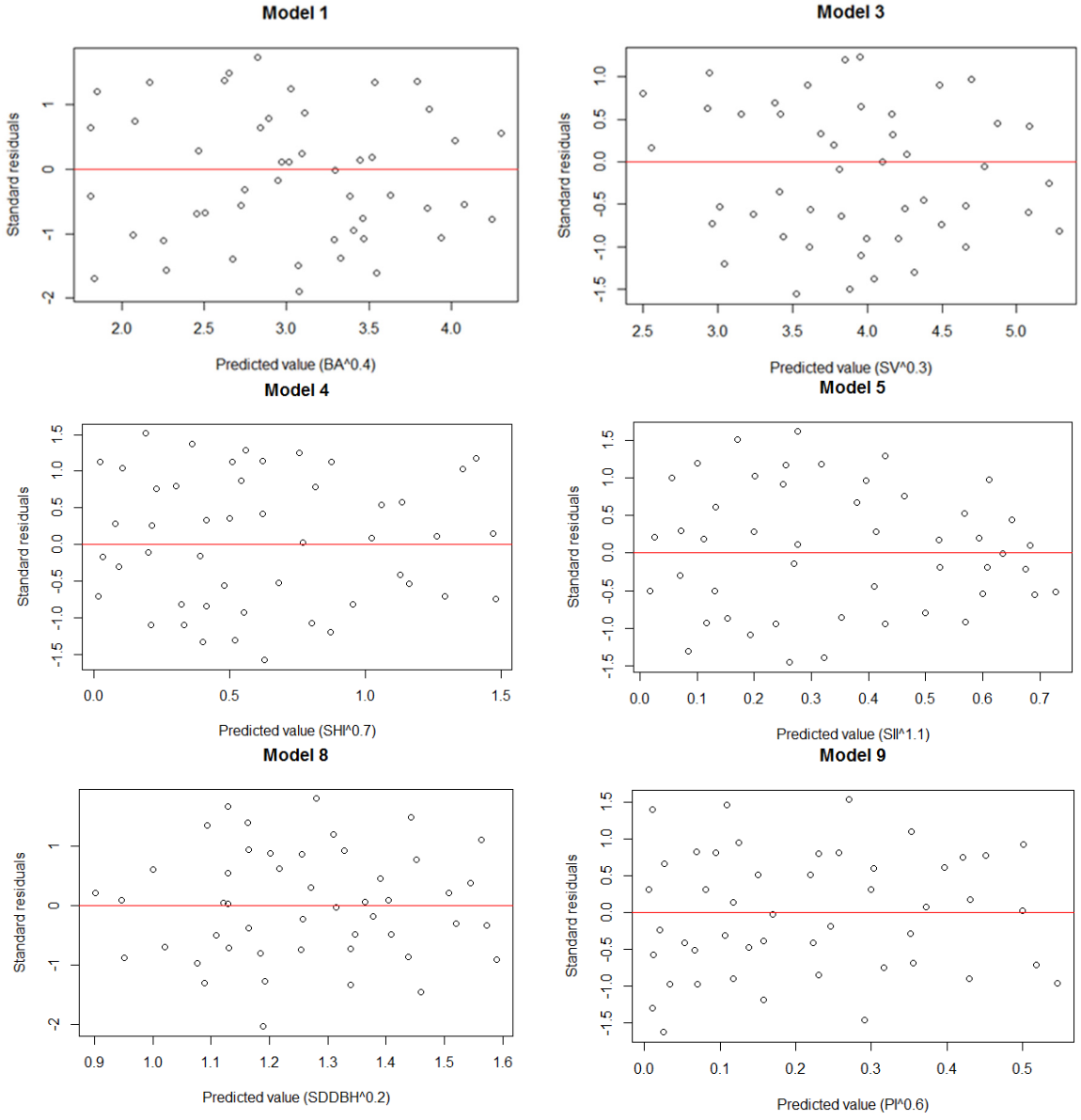

Figure 3. *Cont.*

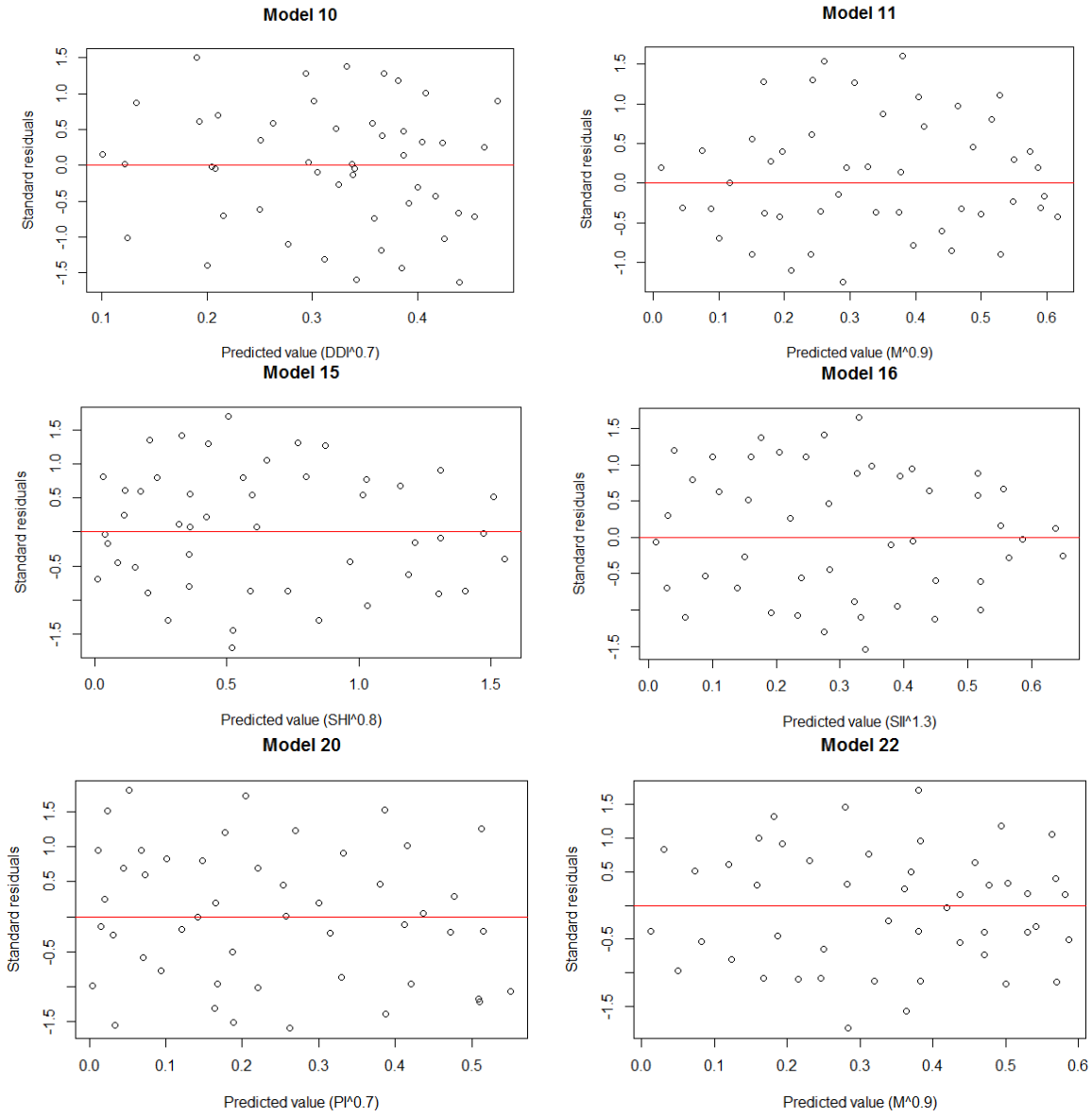

Figure 3. Plots of standardized residuals against the fitted values of the models predicting BA^0.4, SV^0.3, SHI^0.7, SII^1.1, SDDBH^0.2, PI^0.8, DDI^0.7, and $\overline{M}$0.9 (Model 1, 3, 4, 5, 8, 9, 10, and 11, respectively) using spectral and textural measures.

Table 5. Regression model predicting the forest stand variables using only textural measures as independent variables.

Forest Stand Variables	Predictive Model	R^2_{adj}	RMSE	p
Basal area (BA)	Model 13: BA^0.4 = −0.08251· Glcm_mean + 4.70834	0.38	0.951	3.68×10^{-8}
Quadratic mean diameter (QMD)	Model 14: QMD^(−0.3) = 0.340853 −0.00698· Glcm_mean	0.23	0.127	4.466×10^{-5}
Stand volume (SV)	Model 15: SV^0.3 = −0.09075· Glcm_mean + 5.65686	0.40	2.601	5.475×10^{-6}
Shannon–Wiener index (SHI)	Model 16: SHI^0.8 = −0.11179· Glcm_mean + 3.38682	0.62	0.321	3.357×10^{-8}
Simpson's index (SII)	Model 17: SII^1.3= −0.058316· Glcm_mean + 1.741997	0.59	0.169	1.219×10^{-7}
Gini coefficient (GC)	Model 18: GC = 0.3508 − 0.006322· Glcm_mean	0.40	0.052	0.547×10^{-6}
Number of trees (NT)	Model 19: NT^0.6 = 101.5011 − 1.4812· Glcm_mean	0.22	20.214	0.459×10^{-7}
Standard deviation of DBHs (SDDBH)	Model 20: SDDBH^0.2 = −0.0352· Glcm_mean + 2.8799	0.28	0.200	0.0008232
Pielou index (PI)	Model 21: PI^0.7 = −0.041014· Glcm_mean + 1.248652	0.57	0.127	1.964×10^{-7}
Diameter differentiation index (DDI)	Model 22: DDI^0.8 = −0.529751· Glcm_entropy − 0.012799· Glcm_mean − 2.536325· Glcm_ASM + 2.1938	0.41	0.067	0.0003796
Species intermingling index ($\overline{M}$)	Model 23: $\overline{M}$^0.9 = −0.28447· Glcm_entropy − 0.04386· Glcm_mean + 1.94016	0.59	0.160	5.475×10^{-7}
Species intermingling index ($\overline{M}$)	Model 24: $\overline{M}$*^0.9 = 1.577187 − 0.185160· Entropy − 0.034526· Glcm_mean	0.62	0.147	3.235×10^{-6}

* Species intermingling index calculated from all the plots excluding the plots of pure plantation.

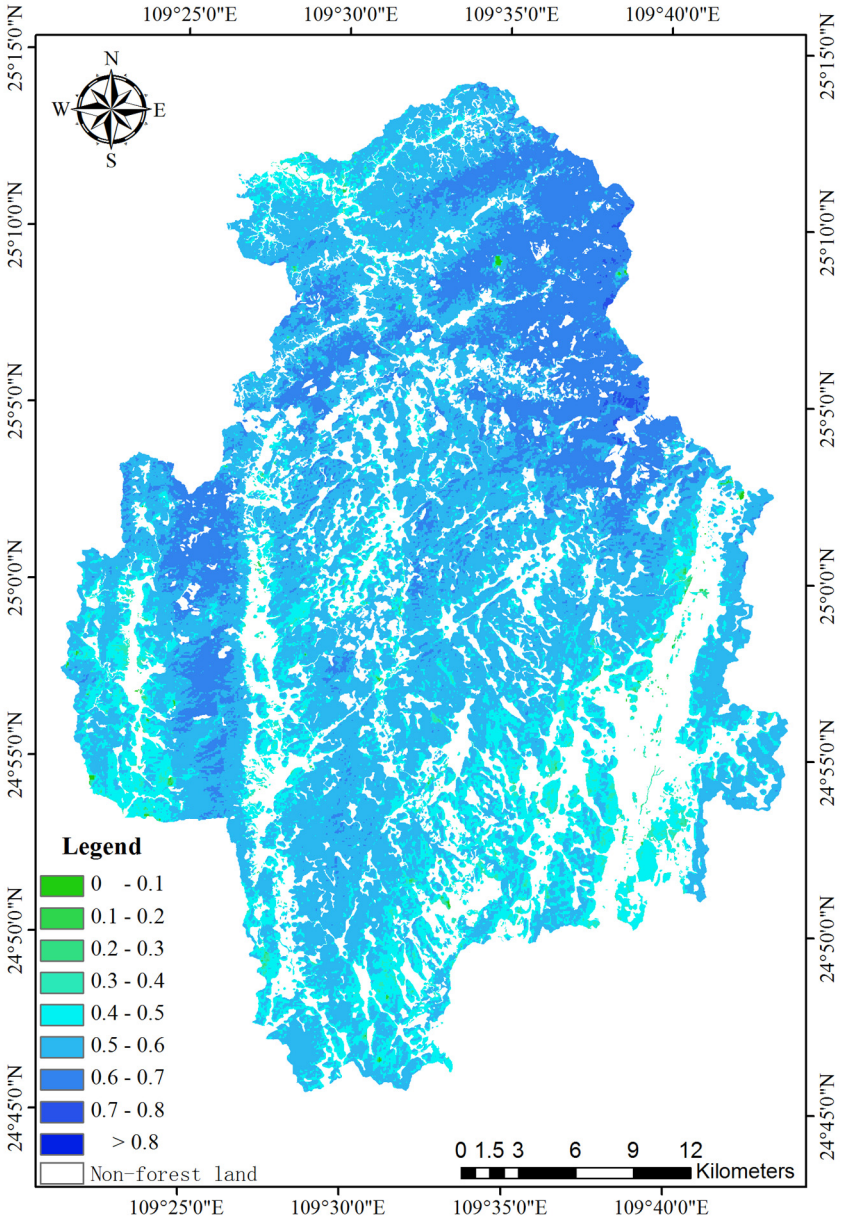

Figure 4. Thematic map of Simpson's index of a county in Guangxi Autonomous Region.

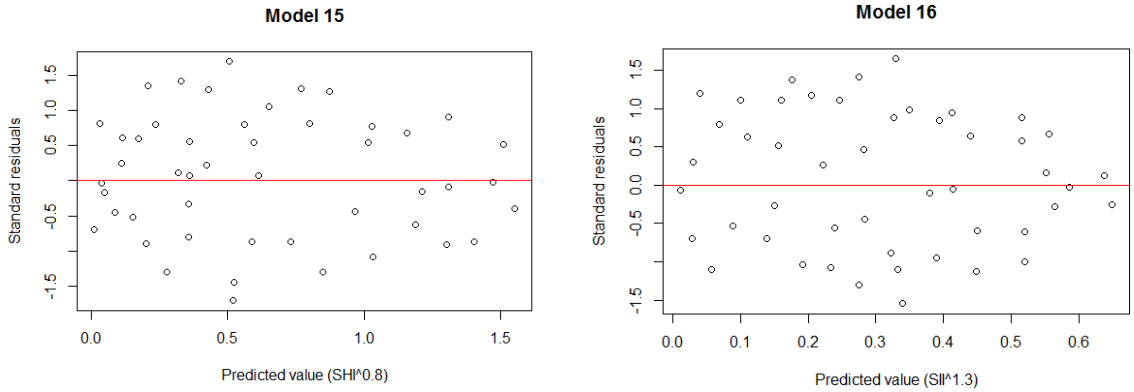

Figure 5. *Cont.*

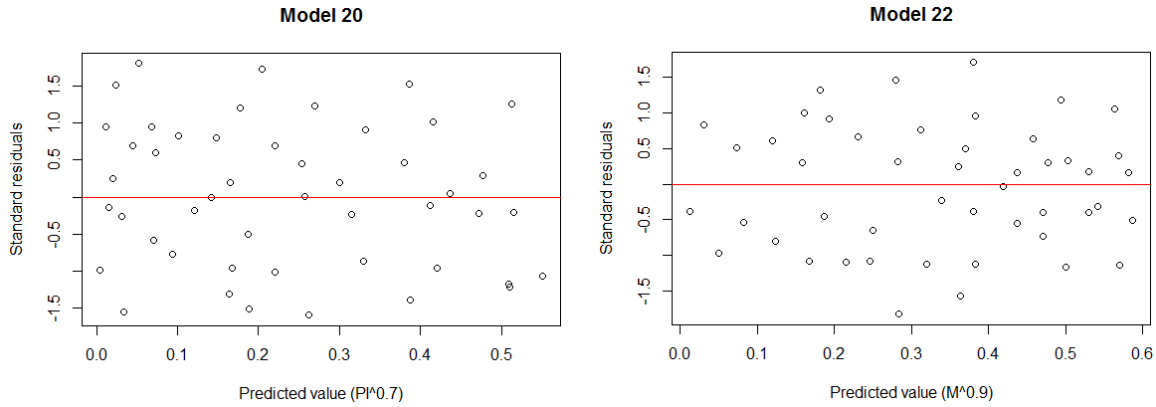

Figure 5. Plots of standardized residuals against the fitted values of the models predicting SII^0.8, SII^1.3, PI^0.7 and $\overline{M}^{0.9}$ (Model 15, 16, 20 and Model 22, respectively) using only textural measures.

4. Discussion

We first built our predictive models using both spectral and textural measures, but only certain spectral measures were retained in the models. This could be attributed to the problems of multicollinearity. The produced models (1, 3, 4, 5, 8, 9, 10, 11 and 12) allowed predictions of the BA, SV, SHI, SII, SDDBH, PI, DDI and $\overline{M}$ (R^2_{adj} values were between 0.50 and 0.70, $p < 0.01$). Vegetation indices were commonly used and promising independent variables in estimation of forest stand variables [55,57]. In the present study, only VI was included in models (9–12), whereas no vegetation indices were included in model (1, 3, 4, 5, 8), though eight vegetation indices were involved as potential regressors to establish the predict models. Similar results were reported by Castillo-Santiago *et al.* [35] who employed four vegetation indices to produce models predicting BA, SV and above ground biomass but found no one was included in the final models. The effectiveness of vegetation indices for predicting forest stand variables was determined by both nature of the forests and the quantity of shadows [35]. For instance, Steininger [58] and Castillo-Santiago *et al.* [35] documented that the best results for spectral information (vegetation indices) to explain variation in forest structure were at lower biomass level. Eckert [59] and Wallner *et al.* [55] explained the effectiveness of the their vegetation indices (e.g., GR and SR) for estimating forest stand variables as follows: a low value for the vegetation indices implies the presence of stands of coniferous forest with shady areas and relatively low stand density, while higher values for these indices imply broadleaved forest with a closed canopy. In the present study, we obtained very low and non-statistically significant correlation coefficients between the forest stand variables and vegetation indices, e.g., GEMI, GR, MSI, and SVR. This might be attributed to the nature of the 48 plots used to produce the models. These plots were of relatively low density and with shady area. Furthermore, most of them were dominated by the coniferous tree species such as *Cunninghamia lanceolata* and *Pinus massoniana*. These features together might result in a very low value of vegetation indices. In addition, multicollinearity might also account for the exclusion of vegetation indices.

None of these models, except model 10, had textural measures as independent variables. In comparison to our results, many studies have demonstrated that the inclusion of textural features, especially second-order textural measures, to spectral measures could improve the estimation of forest stand variables as well as the accuracy of forest classification. For example, Wulder *et al.* [60] found that with the inclusion of texture, the ability to estimate hardwood forest leaf area index (LAI) from remotely sensed imagery increased by approximately 20%. Kim *et al.* [61] reported that the classification accuracy using IKONOS imagery was improved by adding the textural features to the spectral properties. Eckert [1] documented that estimation of tropical rainforest biomass/carbon, based on WorldView-2, exhibited an obvious improvement after introducing textural information to spectral information. The reason why our results are not consistent with these studies might be due to the

relatively lower spatial resolution of the SPOT-5 imagery compared with the very high resolution (VHR) satellite imagery (e.g., IKONOS and Worldview-2 employed in the above-mentioned studies). Lu and Weng [62] argued that the importance of introducing textural information increases as spatial resolution increases. Franklin *et al.* [63] also found that the addition of image texture increased the classification accuracy of high spatial detail imagery (pixel size < 1 m) relative to low spatial detail imagery. Furthermore, the poor significance of textural measures could be attribute to the variables to predict such diversity indices. These diversity indices only measure one dimension of diversity [64], whereas the texture measures included many dimensions. For example, mixture of two pine species could have the same species diversity as a mixture of one pine species and one birch species. The two mixtures would have similar diversity indices but much different texture indices. In this case, the correlation between textural measures and diversity indices would be extremely low.

In addition, the importance of introducing textural measures also depends on the research subject. For instance, Ota *et al.* [65] found that the addition of textural information improved the discrimination of hinoki cypress and cool-temperate mixed forest whereas no improvement for Japanese cedar and a clear cut area was observed. Franklin [66] also documented that the addition of texture generally improved the classification accuracy of hardwood stands, more so than for softwood stands. Using the estimation of structural diversity indices (GC, SDDBH and DDI) for example, Ozdemir and Karnieli [13] explained why the importance of textural measures varied between different research subjects. They stated that the stands in which trees were regularly interspaced and the stem density was high, had lower structural diversity but produced higher textural values. On the contrary, the stands with higher structural diversity produced lower textural values because the large crowns and the gaps in such clumped stands increase the number of adjacent (neighbor) pixels with similar or identical gray levels. In our study, the 48 candidate plots used to build the predictive models varied significantly in terms of species composition and structural characteristics (Table 1). For instance, SHI ranged from 0 to 1.801, indicating the plots consisted of single-tree species plantations and mixed-species forests. SV ranged from 21.02 m^3/ha to 263.13 m^3/ha, producing a coefficient of variance (CV) of 57.10%. The high variation of these 48 plots may have changed the relationship between the textural measures and the forest stand variables when we combined them for regression analysis, which might also account for the exclusion of textural measures when developing the predictive models. As a result, prior to model development, it seemed to be quite necessary to stratify the forest inventory plots into sub-categories (e.g., pure plantation and mixed-tree species forests) for which subsequent regression analysis should be done separately.

This assumption was supported by our findings that the R^2_{adj} would increase from 0.59 to 0.62 (Table 5) if we built the model predicting $\overline{M}$ using all data excluding those from the pure plantation. Actually, many other studies have already demonstrated the efficiency of classification/stratification in building such predictive models. For example, Eckert [1] reported that the estimation of tropical rainforest biomass/carbon could be improved by developing and applying forest stratum-specific models. Wallner *et al.* [55] firstly stratified forest inventory plots based on forest types and then produced separate predictive models and found that stratification improved the regression models. Similarly, we also produced the models for the other stand variables using all data excluding those from the pure plantation; however, no significant/obvious improvement was observed for R^2_{adj}, in contrast to $\overline{M}$. Therefore, these are not listed in Tables 4 and 5. We might conclude that amongst the predicted variables in the present study, $\overline{M}$ was the most sensitive to the image information. This might be attributed to the much more detailed information that $\overline{M}$ provided compared with the other forest stand variables. For instance, BA and SV contained neither species composition nor tree position information. SHI and SII did not involve tree position information, though they accounted for tree species composition. In addition, although two stands had similar diversity indices, they would differ with respect to image textural measures. For example, mixture of two pine species could have the same species diversity as a mixture of one pine species and one birch species. The two mixtures would

have similar diversity indices but much different texture indices. In contrast, $\overline{M}$ involved both species composition and tree position information and could be better represented by textural measures.

In addition, we also developed the models with only textural measures as independent variables for comparison purposes because some published literature has shown that textural measures alone were also promising for the prediction of forest stand variables. For instance, based on IKONOS satellite data, Kayitakire *et al.* [67] and Gebreslasie [52] succeeded in developing reliable models predicting conventional forest variables using only textural features. Our results indicated that amongst the 11 candidate forest stand variables (dependent variables), only species diversity represented by SHI, PI and SII could be reliably estimated using only textural measures (R^2_{adj} values for SHI, PI and SII were 0.62, 0.57 and 0.59, respectively ($p < 0.01$)). Actually, the relationship between species diversity and textural measures has been explored by many authors in varying research fields. For instance, a similar result was reported by Nagendra *et al.* [68], who also found that the textural measures were significantly correlated with tree species diversity measured by species richness and the Shannon index. St-Louis *et al.* [69] and wood *et al.* [70], who tested image texture as a predictor of bird species richness and density, concluded that textural measures are very promising predictors and even perform better than field-measured vegetation structure. Magurran [36] classified diversity as either species richness measures or heterogeneity measures. Heterogeneity measures such SHI, PI and SII are those that combine the component diversity of the richness and evenness measures and are hence regarded to represent considerably more information [36,71,72]. The rich information of the heterogeneity measures (e.g., SHI, PI and SII in the present study) might account for their high sensitivity to remotely sensed image texture, which was regarded as a surrogate for vegetation structure [70]. Furthermore, Gallardo-Cruz *et al.* [73] argued that compared with first-order texture, the second-order texture had greater potential to reflect the heterogeneity of forest stands as it considers pixel-neighbor relationships. Their statement is supported by our t predicting SHI, PI and SII, whose independent variable was Glcm_mean (second-order texture).

In terms of the forest stand variables to be predicted, most studies focused on the estimation of conventional forest stand variables such as SV, NT, BA, and QMD using remotely sensed data [35,55,74,75]. Only a few studies have investigated the extraction of the more complex structural variables such as tree size diversity and tree position diversity [13,76,77]. However, these complex structural variables are significant in the development of management plans, especially for multipurpose forests, and are usually more expensive and time-consuming to collect in a field survey. In addition, the complexity of such structural variables was further introduced by the spatial and temporal scale at which they should be investigated. For instance, Lamonaca *et al.* [77] argued that these complex structural variables representing spatial heterogeneity should be detected across scales since it was not possible to infer the multiple-scale structural and dynamical patterns from a system description that spanned only a narrow window of resolution [78]. They therefore compared three-level segmentation and demonstrated that multi-resolution segmentation was able to delineate scale-dependent patterns of forest structural heterogeneity, even in an initial stage of old-growth structural differentiation. Their findings have a potential to improve the sampling design of field surveys aimed at characterizing forest structural complexity across multiple spatio-temporal scales. In the present study, in addition to the conventional forest variables, we also succeeded in producing models allowing us to forecast the more complex forest structure, *i.e.*, tree size diversity represented by SDDBH, and tree position diversity represented by $\overline{M}$. The tree size diversity affected the economical, ecological as well as social values and hence provided important information for prescribing management regimes [15]. The tree position diversity was not only used to infer ecological mechanisms [79,80] but was also of practical importance, e.g., formulation of tree-level harvest optimization [17] and identification of the optimal tree species arrangement for enrichment planting [81]. In the present study, the predictive models predicting these complex structural variables was unfortunately built without taking the concept of multiple-scale analysis and hierarchy. Following the findings of Lamonaca *et al.* [77], it might be necessary to first conduct multi-resolution segmentation

and then produce the predictive models for the segments which had the same structural variables if the training data (field plots) was sufficient. In addition, the predictive models were developed using only three SPOT-5 images and hence it was not safe to apply across the entire Guangxi Zhuang Autonomous Region. However, thematic maps could be reliably produced within the research area for which the models were built. Furthermore, non-compatibility of the produced models might be introduced because each forest variables were predicted independently. For instance, BA, QMD and NT were related by BA = QMD × QMD × NT × 0.00007854 (given BA in m^2/ha, QMD in cm and NT in trees/ha). Because of non-compatibility, the estimated BA might differ from the value produced above. Therefore compatible models should be encouraged to develop. We also could have negative predictions. For example, the first five smallest values for VI were 1.278, 1.307, 1.311, 1.317 and 1.320. If model 11 were employed for prediction, we would get four negative predictions, *i.e.*, −0.177, −0.046, −0.028 and −0.003, which were close to zero. Actually, the plots with the species intermingling index around zero (no matter positive or negative) were all pure plantation. Therefore, if we get the negative predictions, we could assign them to pure plantation.

Multiple linear regression was commonly employed in forestry researches. For instance, it was widely used to produce forest growth and yield models [82–85]. Also, like this present study, it was normally performed to extract forest stand variables using remotely sensed data [13,35,55,66,86,87]. However, this statistical technique was criticized for its limitations. For example, Gebreslasie *et al.* [52], Dye *et al.* [88] and Lottering and Mutanga [89] documented that multiple linear regression assumed both linearity and independence between variables, which was seldom observed in forest and remotely sensed data. Furthermore, linear regression also required the absence of collinearity amongst input variables [88,90]. VIF was normally employed to analyze multicollinearity and some variables indicating on collinearity (multicollinearity) might be removed, which resulted in model that explained less variance than the best possible full model with more variables. Therefore, more robust statistical methods, which did not need to make any assumptions about the data, such as artificial Neural Networks (ANN) [89–91], Classification and Regression Tree Analysis (CART) [22,92,93], and Random forests (RF) [88,94,95] were widely used to investigate complex relationship between forests stand variables and remotely sensed data. These robust statistical techniques should be given first priority in future remote sensing studies as many researches have already demonstrated that nonlinear interactions might exist between the observed data and remotely sensed data [88,90,96]. Even within these robust statistical techniques, they presented different performance in producing the predictive models. For instance, Breiman [97] documented that CART was sensitive to small variations in the training dataset, which could cause instability with regard to variable selection and can adversely affect the predictive performance of the final model [98]. Correspondingly, Dye *et al.* [88] recommended RF to reduce the instability of single regression trees and improve the overall predictive performance. Therefore, studies comparing different statistical techniques for predicting forest stand variables using remotely sensed data should be encouraged. Although the R^2 was a frequently employed efficiency criteria to identify the optimum models and the models with R^2 equal to or more than 0.5 were normally regarded to be reliable [13,25], it might still be reputable since in certain cases models with very low R^2 were also useful for prediction. Actually in addition to R^2, there were also other efficiency criteria such as Nash-Sutcliffe efficiency and Index of agreement, which placed different emphasis on different types of simulated and observed behaviors [99,100]. Janssen and Heuberger [101] documented that the selection of the best efficiency measures should reflect the intended use of the model and should concern model quantities which are deemed relevant for the study at hand. Krause *et al.* [99] recommended a combination of different efficiency criteria for scientific sound model calibration and validation after examining the utility of several efficiency criteria.

Uneven-aged forest management with various objectives has received more attention as a silvicultural alternative in the past few years [2,15,83,102]. In this context, much more detailed information concerning complex forests is needed for management decision-making. Corona [12] considered new paradigms in large-scale monitoring and assessment of forest ecosystems under the

changing perspectives and made commented discussions with examples from the literature produced in the last decade. Remote sensing techniques with various sensors of different spatial and spectral resolutions provide a promising opportunity to extract such detailed information. Therefore, further investigation exploring the relationship between these complex structural indices and the indices derived from different remotely sensed data should be encouraged.

5. Conclusions

Forest structural diversity indices were of great importance to the management of uneven-aged forests. However, they were time consuming and expensive to obtain. In the present study, we have successfully built the predictive models predicting forest structural diversity indices, *i.e.*, Shannon-Wiener index, Simpson's index, Standard deviation of DBHs, Pielou index, Diameter differentiation index and Species intermingling index using both spectral and textural measures. In addition, we also produced models estimating basal area and stand volume. The predictive models would contribute to the formulation of forest management strategy, especially for uneven-aged forests in the context of climate change. Although the produced predictive models provided us a quick and economical estimation of forest structural diversity, they should be applied with great care as biased estimation might occur if we employ them beyond the scope that we developed them. It was noteworthy that multiple linear regression assumed both linearity and independence between variables, which was seldom observed in forest and remotely sensed data. The robust statistical methods, e.g., machine learning, need to perform in future research.

Acknowledgments: This study was supported by the National Natural Science Foundation of China (31370635), the project National Science and Technology Major Projects of China (21-Y30B05-9001-13/15) and the National Natural Science Foundation of China (31300532). We thank the Survey & Planning Institute of State Forestry Administration, China for their data support during our research.

Author Contributions: All authors have made significant contributions to the manuscript. Jinghui Meng and Shiming Li conceived, designed and performed the experiments; Shiming Li, Wei Wang, Qingwang Liu and Shiqin Xie processed the remote sensing data and derived the remote sensing parameters responding to the field plots; Jinghui Meng, Qingwang Liu, and Shiqin Xie analyzed the data and results; Wei Wang contributed reagents/materials/analysis tools; and Jinghui Meng and Shiming Li are the main authors who developed and revised the manuscript; Wu Ma conducted the English Editing.

Conflicts of Interest: The authors declare no conflict of interest.

References

1. Eckert, S. Improved forest biomass and carbon estimations using texture measures from WorldView-2 satellite data. *Remote Sens.* **2012**, *4*, 810–829. [CrossRef]
2. Meng, J.; Lu, Y.; Zeng, J. Transformation of a degraded pinus massoniana plantation into a mixed-species irregular forest: Impacts on stand structure and growth in southern China. *Forests* **2014**, *5*, 3199–3221. [CrossRef]
3. Gärtner, S.; Reif, A. The impact of forest transformation on stand structure and ground vegetation in the southern black forest, germany. *Plant Soil* **2004**, *264*, 35–51. [CrossRef]
4. Chauvat, M.; Titsch, D.; Zaytsev, A.S.; Wolters, V. Changes in soil faunal assemblages during conversion from pure to mixed forest stands. *For. Ecol. Manag.* **2011**, *262*, 317–324. [CrossRef]
5. O'Hara, K.L. The silviculture of transformation—A commentary. *For. Ecol. Manag.* **2001**, *151*, 81–86. [CrossRef]
6. Buongiorno, J. Quantifying the implications of transformation from even to uneven-aged forest stands. *For. Ecol. Manag.* **2001**, *151*, 121–132. [CrossRef]
7. Fürstenau, C.; Badeck, F.W.; Lasch, P.; Lexer, M.J.; Lindner, M.; Mohr, P.; Suckow, F. Multiple-use forest management in consideration of climate change and the interests of stakeholder groups. *Eur. J. For. Res.* **2007**, *126*, 225–239. [CrossRef]
8. Puettmann, K.J.; Wilson, S.M.; Baker, S.C.; Donoso, P.J.; Drössler, L.; Amente, G.; Harvey, B.D.; Knoke, T.; Lu, Y.; Nocentini, S. Silvicultural alternatives to conventional even-aged forest management-what limits global adoption? *For. Ecosyst.* **2015**, *2*, 1–16. [CrossRef]

9. Messier, C.; Puettmann, K.J.; Coates, K.D. *Managing Forests as Complex Adaptive Systems: Building Resilience to the Challenge of Global Change*; Routledge: London, UK, 2013.
10. Filotas, E.; Parrott, L.; Burton, P.J.; Chazdon, R.L.; Coates, K.D.; Coll, L.; Haeussler, S.; Martin, K.; Nocentini, S.; Puettmann, K.J. Viewing forests through the lens of complex systems science. *Ecosphere* **2014**, *5*, 1–23. [CrossRef]
11. Warfield, J.N. *An Introduction to Systems Science*; World Scientific Publishing Co., Inc.: Hackensack, NJ, USA, 2006.
12. Corona, P. Consolidating new paradigms in large-scale monitoring and assessment of forest ecosystems. *Environ. Res.* **2016**, *144*, 8–14. [CrossRef] [PubMed]
13. Ozdemir, I.; Karnieli, A. Predicting forest structural parameters using the image texture derived from worldview-2 multispectral imagery in a dryland forest, israel. *Int. J. Appl. Earth Obs. Geoinform.* **2011**, *13*, 701–710. [CrossRef]
14. Pommerening, A. Approaches to quantifying forest structures. *Forestry* **2002**, *75*, 305–324. [CrossRef]
15. Lexerød, N.L.; Eid, T. An evaluation of different diameter diversity indices based on criteria related to forest management planning. *For. Ecol. Manag.* **2006**, *222*, 17–28. [CrossRef]
16. O'Hara, K. *Multiaged Silviculture: Managing for Complex Forest Stand Structures*; Oxford University Press: Oxford, UK, 2014.
17. Bettinger, P.; Tang, M. Tree-level harvest optimization for structure-based forest management based on the species mingling index. *Forests* **2015**, *6*, 1121–1144. [CrossRef]
18. Lei, X.; Tang, M.; Lu, Y.; Hong, L.; Tian, D. Forest inventory in China: Status and challenges. *Int. For. Rev.* **2009**, *11*, 52–63. [CrossRef]
19. Corona, P.; Chirici, G.; McRoberts, R.E.; Winter, S.; Barbati, A. Contribution of large-scale forest inventories to biodiversity assessment and monitoring. *For. Ecol. Manag.* **2011**, *262*, 2061–2069. [CrossRef]
20. Corona, P.; Marchetti, M. Outlining multi-purpose forest inventories to assess the ecosystem approach in forestry. *Plant Biosyst.* **2007**, *141*, 243–251. [CrossRef]
21. Winter, S.; Chirici, G.; McRoberts, R.E.; Hauk, E. Possibilities for harmonizing national forest inventory data for use in forest biodiversity assessments. *Forestry* **2008**, *81*, 33–44. [CrossRef]
22. Gómez, C.; Wulder, M.A.; Montes, F.; Delgado, J.A. Modeling forest structural parameters in the mediterranean pines of central spain using QuickBird-2 imagery and classification and regression tree analysis (CART). *Remote Sens.* **2012**, *4*, 135–159. [CrossRef]
23. Tanaka, S.; Takahashi, T.; Nishizono, T.; Kitahara, F.; Saito, H.; Iehara, T.; Kodani, E.; Awaya, Y. Stand volume estimation using the k-NN technique combined with forest inventory data, satellite image data and additional feature variables. *Remote Sens.* **2014**, *7*, 378–394. [CrossRef]
24. McRoberts, R.E.; Tomppo, E.O. Remote sensing support for national forest inventories. *Remote Sens. Environ.* **2007**, *110*, 412–419. [CrossRef]
25. Wolter, P.T.; Townsend, P.A.; Sturtevant, B.R. Estimation of forest structural parameters using 5 and 10 m SPOT-5 satellite data. *Remote Sens. Environ.* **2009**, *113*, 2019–2036. [CrossRef]
26. Popescu, S.C.; Wynne, R.H.; Nelson, R.F. Measuring individual tree crown diameter with LiDAR and assessing its influence on estimating forest volume and biomass. *Can. J. Remote Sens.* **2003**, *29*, 564–577. [CrossRef]
27. Tsui, O.W.; Coops, N.C.; Wulder, M.A.; Marshall, P.L.; McCardle, A. Using multi-frequency radar and discrete-return LiDAR measurements to estimate above-ground biomass and biomass components in a coastal temperate forest. *ISPRS J. Photogramm. Remote Sens.* **2012**, *69*, 121–133. [CrossRef]
28. Meyer, V.; Saatchi, S.; Poulsen, J.; Clark, C.; Lewis, S.; White, L. LiDAR estimation of aboveground biomass in a tropical coastal forest of gabon. *AGU Fall Meet. Abstr.* **2012**, *1*, 0440.
29. Suárez, J.C.; Ontiveros, C.; Smith, S.; Snape, S. Use of airborne LiDAR and aerial photography in the estimation of individual tree heights in forestry. *Comput. Geosci.* **2005**, *31*, 253–262. [CrossRef]
30. Kwak, D.-A.; Lee, W.-K.; Lee, J.-H.; Biging, G.S.; Gong, P. Detection of individual trees and estimation of tree height using LiDAR data. *J. For. Res.* **2007**, *12*, 425–434. [CrossRef]
31. Unger, D.R.; Hung, I.-K.; Brooks, R.; Williams, H. Estimating number of trees, tree height and crown width using LiDAR data. *GISci. Remote Sens.* **2014**, *51*, 227–238. [CrossRef]
32. Koch, B.; Heyder, U.; Weinacker, H. Detection of individual tree crowns in airborne LiDAR data. *Photogramm. Eng. Remote Sens.* **2006**, *72*, 357–363. [CrossRef]

33. Jing, L.; Hu, B.; Li, J.; Noland, T. Automated delineation of individual tree crowns from LiDAR data by multi-scale analysis and segmentation. *Photogramm. Eng. Remote Sens.* **2012**, *78*, 1275–1284. [CrossRef]
34. Chang, A.; Eo, Y.; Kim, Y.; Kim, Y. Identification of individual tree crowns from LiDAR data using a circle fitting algorithm with local maxima and minima filtering. *Remote Sens. Lett.* **2013**, *4*, 29–37. [CrossRef]
35. Castillo-Santiago, M.A.; Ricker, M.; de Jong, B.H. Estimation of tropical forest structure from spot-5 satellite images. *Int. J. Remote Sens.* **2010**, *31*, 2767–2782. [CrossRef]
36. Magurran, A.E. *Measuring Biological Diversity*; John Wiley & Sons: New York, NY, USA, 2013.
37. Li, Y.; Hui, G.; Zhao, Z.; Hu, Y. The bivariate distribution characteristics of spatial structure in natural korean pine broad-leaved forest. *J. Veg. Sci.* **2012**, *23*, 1180–1190. [CrossRef]
38. Hui, G.; Kv, G.; Hu, Y.; Chen, B. Characterizing forest spatial distribution pattern with the mean value of uniform angle index. *Acta Ecol. Sin.* **2003**, *24*, 1225–1229.
39. Gangying, H.; von Gadow, K.; Albert, M. The neighbourhood pattern—A new structure parameter for describing distribution of forest tree position. *Sci. Silvae Sin.* **1999**, *35*, 37–42.
40. Yan-bo, H.; Gang-ying, H. A discussion on forest management method optimizing forest spatial structure. *For. Res.* **2006**, *19*, 1–4.
41. Gangying, H.; Li, L.; Zhonghua, Z.; Puxing, D. Comparison of methods in analysis of the tree spatial distribution pattern. *Acta Ecol. Sin.* **2007**, *27*, 4717–4728. [CrossRef]
42. Pommerening, A.; Stoyan, D. Edge-correction needs in estimating indices of spatial forest structure. *Can. J. For. Res.* **2006**, *36*, 1723–1739. [CrossRef]
43. Germany, Trimble. *eCognition Developer 7 Reference Book*; Trimble Germany: Munich, Germany, 2011.
44. Rouse, J.W., Jr.; Haas, R.; Schell, J.; Deering, D. Monitoring vegetation systems in the great plains with ERTS. *Third Earth Resources Technology Satellite-1 Symposium- Volume I: Technical Presentations*; NASA SP-351; NASA: Washington, DC, USA, 1974; p. 309.
45. Jordan, C.F. Derivation of leaf-area index from quality of light on the forest floor. *Ecology* **1969**, *50*, 663–666. [CrossRef]
46. Lyon, J.G.; Yuan, D.; Lunetta, R.S.; Elvidge, C.D. A change detection experiment using vegetation indices. *Photogramm. Eng. Remote Sens.* **1998**, *64*, 143–150.
47. Kanemasu, E. Seasonal canopy reflectance patterns of wheat, sorghum, and soybean. *Remote Sens. Environ.* **1974**, *3*, 43–47. [CrossRef]
48. Huete, A.R. A soil-adjusted vegetation index (SAVI). *Remote Sens. Environ.* **1988**, *25*, 295–309. [CrossRef]
49. Verstraete, M.M.; Pinty, B. Designing optimal spectral indexes for remote sensing applications. *IEEE Trans. Geosci. Remote Sens.* **1996**, *34*, 1254–1265. [CrossRef]
50. Ouma, Y.O.; Ngigi, T.; Tateishi, R. On the optimization and selection of wavelet texture for feature extraction from high-resolution satellite imagery with application towards urban-tree delineation. *Int. J. Remote Sens.* **2006**, *27*, 73–104. [CrossRef]
51. Song, C.; Dickinson, M.B.; Su, L.; Zhang, S.; Yaussey, D. Estimating average tree crown size using spatial information from ikonos and quickbird images: Across-sensor and across-site comparisons. *Remote Sens. Environ.* **2010**, *114*, 1099–1107. [CrossRef]
52. Gebreslasie, M.; Ahmed, F.; van Aardt, J.A. Extracting structural attributes from IKONOS imagery for eucalyptus plantation forests in Kwazulu-Natal, South Africa, using image texture analysis and artificial neural networks. *Int. J. Remote Sens.* **2011**, *32*, 7677–7701. [CrossRef]
53. Shaban, M.; Dikshit, O. Improvement of classification in urban areas by the use of textural features: The case study of Lucknow City, Uttar Pradesh. *Int. J. Remote Sens.* **2001**, *22*, 565–593. [CrossRef]
54. Sheather, S. *A Modern Approach to Regression with R*; Springer: Berlin, Germany, 2009.
55. Wallner, A.; Elatawneh, A.; Schneider, T.; Knoke, T. Estimation of forest structural information using rapideye satellite data. *Forestry* **2015**, *88*, 96–107. [CrossRef]
56. State Forestry Administration of the People's Republic of China. The 8th forest resources inventory results. *For. Res. Manag.* **2014**, *1*, 1–2.
57. Jensen, J.R. *Introductory Digital Image Processing: A Remote Sensing Perspective*; Pearson College Division: Englewood Cliff, NJ, USA, 2005.
58. Steininger, M. Satellite estimation of tropical secondary forest above-ground biomass: Data from Brazil and Bolivia. *Int. J. Remote Sens.* **2000**, *21*, 1139–1157. [CrossRef]

59. Eckert, S. *A Contribution to Sustainable Forest Management in Patagonia: Object-Oriented Classification and Forest Parameter Extraction Based on Aster and Ladsat ETM+ Data*; Remote Sensing Laboratories, Department of Geography, University of Zurich: Zurich, Switzerland, 2006.
60. Wulder, M.A.; LeDrew, E.F.; Franklin, S.E.; Lavigne, M.B. Aerial image texture information in the estimation of northern deciduous and mixed wood forest leaf area index (LAI). *Remote Sens. Environ.* **1998**, *64*, 64–76. [CrossRef]
61. Kim, M.; Madden, M.; Warner, T.A. Forest type mapping using object-specific texture measures from multispectral Ikonos imagery. *Photogramm. Eng. Remote Sens.* **2009**, *75*, 819–829. [CrossRef]
62. Lu, D.; Weng, Q. A survey of image classification methods and techniques for improving classification performance. *Int. J. Remote Sens.* **2007**, *28*, 823–870. [CrossRef]
63. Franklin, S.; Wulder, M.; Gerylo, G. Texture analysis of IKONOS panchromatic data for Douglas-fir forest age class separability in British Columbia. *Int. J. Remote Sens.* **2001**, *22*, 2627–2632. [CrossRef]
64. Li, Y.; Hui, G.; Zhao, Z.; Hu, Y.; Ye, S. Spatial structural characteristics of three hardwood species in Korean pine broad-leaved forest—Validating the bivariate distribution of structural parameters from the point of tree population. *For. Ecol. Manag.* **2014**, *314*, 17–25. [CrossRef]
65. Ota, T.; Mizoue, N.; Yoshida, S. Influence of using texture information in remote sensed data on the accuracy of forest type classification at different levels of spatial resolution. *J. For. Res.* **2011**, *16*, 432–437. [CrossRef]
66. Franklin, S.; Hall, R.; Moskal, L.; Maudie, A.; Lavigne, M. Incorporating texture into classification of forest species composition from airborne multispectral images. *Int. J. Remote Sens.* **2000**, *21*, 61–79. [CrossRef]
67. Kayitakire, F.; Giot, P.; Defourny, P. Automated delineation of the forest stands using digital color orthophotos: Case study in Belgium. *Can. J. Remote Sens.* **2002**, *28*, 629–640. [CrossRef]
68. Nagendra, H.; Rocchini, D.; Ghate, R.; Sharma, B.; Pareeth, S. Assessing plant diversity in a dry tropical forest: Comparing the utility of landsat and ikonos satellite images. *Remote Sens.* **2010**, *2*, 478–496. [CrossRef]
69. St-Louis, V.; Pidgeon, A.M.; Radeloff, V.C.; Hawbaker, T.J.; Clayton, M.K. High-resolution image texture as a predictor of bird species richness. *Remote Sens. Environ.* **2006**, *105*, 299–312. [CrossRef]
70. Wood, E.M.; Pidgeon, A.M.; Radeloff, V.C.; Keuler, N.S. Image texture predicts avian density and species richness. *PLoS ONE* **2013**, *8*, e63211.
71. Newton, A.C. *Forest Ecology and Conservation: A Handbook of Techniques*; Oxford University Press: Oxford, UK, 2007.
72. Schneider, D.C. *Quantitative Ecology: Measurement, Models and Scaling*; Academic Press: Cambridge, MA, USA, 2009.
73. Gallardo-Cruz, J.A.; Meave, J.A.; González, E.J.; Lebrija-Trejos, E.E.; Romero-Romero, M.A.; Pérez-García, E.A.; Gallardo-Cruz, R.; Hernández-Stefanoni, J.L.; Martorell, C. Predicting tropical dry forest successional attributes from space: Is the key hidden in image texture? *PLoS ONE* **2012**, *7*, e30506–e30512. [CrossRef] [PubMed]
74. Couteron, P.; Pelissier, R.; Nicolini, E.A.; Paget, D. Predicting tropical forest stand structure parameters from fourier transform of very high-resolution remotely sensed canopy images. *J. Appl. Ecol.* **2005**, *42*, 1121–1128. [CrossRef]
75. Mora, B.; Wulder, M.A.; White, J.C.; Hobart, G. Modeling stand height, volume, and biomass from very high spatial resolution satellite imagery and samples of airborne LiDAR. *Remote Sens.* **2013**, *5*, 2308–2326. [CrossRef]
76. Ozdemir, I.; Norton, D.A.; Ozkan, U.Y.; Mert, A.; Senturk, O. Estimation of tree size diversity using object oriented texture analysis and aster imagery. *Sensors* **2008**, *8*, 4709–4724. [CrossRef]
77. Lamonaca, A.; Corona, P.; Barbati, A. Exploring forest structural complexity by multi-scale segmentation of VHR imagery. *Remote Sens. Environ.* **2008**, *112*, 2839–2849. [CrossRef]
78. Parrott, L. Complexity and the limits of ecological engineering. *Trans. Am. Soc. Agric. Eng.* **2002**, *45*, 1697–1702. [CrossRef]
79. He, F.; Duncan, R.P. Density-dependent effects on tree survival in an old-growth Douglas fir forest. *J. Ecol.* **2000**, *88*, 676–688. [CrossRef]
80. Getzin, S.; Dean, C.; He, F.; Trofymow, J.A.; Wiegand, K.; Wiegand, T. Spatial patterns and competition of tree species in a Douglas-fir chronosequence on vancouver island. *Ecography* **2006**, *29*, 671–682. [CrossRef]
81. Hao, Z.; Zhang, J.; Song, B.; Ye, J.; Li, B. Vertical structure and spatial associations of dominant tree species in an old-growth temperate forest. *For. Ecol. Manag.* **2007**, *252*, 1–11. [CrossRef]

82. Sánchez-González, M.; del Río, M.; Cañellas, I.; Montero, G. Distance independent tree diameter growth model for cork oak stands. *For. Ecol. Manag.* **2006**, *225*, 262–270. [CrossRef]
83. Condés, S.; Sterba, H. Comparing an individual tree growth model for pinus halepensis mill. In the Spanish region of murcia with yield tables gained from the same area. *European J. For. Res.* **2008**, *127*, 253–261. [CrossRef]
84. Zhao, D.; Borders, B.; Wilson, M. Individual-tree diameter growth and mortality models for bottomland mixed-species hardwood stands in the lower mississippi alluvial valley. *For. Ecol. Manag.* **2004**, *199*, 307–322. [CrossRef]
85. Pukkala, T.; Lähde, E.; Laiho, O. Growth and yield models for uneven-sized forest stands in Finland. *For. Ecol. Manag.* **2009**, *258*, 207–216. [CrossRef]
86. Kayitakire, F.; Hamel, C.; Defourny, P. Retrieving forest structure variables based on image texture analysis and IKONOS-2 imagery. *Remote Sens. Environ.* **2006**, *102*, 390–401. [CrossRef]
87. Andersen, H.-E.; McGaughey, R.J.; Reutebuch, S.E. Estimating forest canopy fuel parameters using LiDAR data. *Remote Sens. Environ.* **2005**, *94*, 441–449. [CrossRef]
88. Dye, M.; Mutanga, O.; Ismail, R. Combining spectral and textural remote sensing variables using random forests: Predicting the age of pinus patula forests in Kwazulu-Natal, South Africa. *J. Spat. Sci.* **2012**, *57*, 193–211. [CrossRef]
89. Lottering, R.; Mutanga, O. Estimating the road edge effect on adjacent eucalyptus grandis forests in Kwazulu-Natal, South Africa, using texture measures and an artificial neural network. *J. Spat. Sci.* **2012**, *57*, 153–173. [CrossRef]
90. Jensen, J.; Qiu, F.; Ji, M. Predictive modelling of coniferous forest age using statistical and artificial neural network approaches applied to remote sensor data. *Int. J. Remote Sens.* **1999**, *20*, 2805–2822.
91. Ingram, J.C.; Dawson, T.P.; Whittaker, R.J. Mapping tropical forest structure in southeastern Madagascar using remote sensing and artificial neural networks. *Remote Sens. Environ.* **2005**, *94*, 491–507. [CrossRef]
92. Lobell, D.B.; Ortiz-Monasterio, J.I.; Asner, G.P.; Naylor, R.L.; Falcon, W.P. Combining field surveys, remote sensing, and regression trees to understand yield variations in an irrigated wheat landscape. *Agron. J.* **2005**, *97*, 241–249.
93. Chubey, M.S.; Franklin, S.E.; Wulder, M.A. Object-based analysis of IKONOS-2 imagery for extraction of forest inventory parameters. *Photogramm. Eng. Remote Sens.* **2006**, *72*, 383–394. [CrossRef]
94. Yu, X.; Hyyppä, J.; Vastaranta, M.; Holopainen, M.; Viitala, R. Predicting individual tree attributes from airborne laser point clouds based on the random forests technique. *ISPRS J. Photogramm. Remote Sens.* **2011**, *66*, 28–37. [CrossRef]
95. Baccini, A.; Friedl, M.; Woodcock, C.; Warbington, R. Forest biomass estimation over regional scales using multisource data. *Geophys. Res. Lett.* **2004**, *31*. [CrossRef]
96. De'ath, G.; Fabricius, K.E. Classification and regression trees: A powerful yet simple technique for ecological data analysis. *Ecology* **2000**, *81*, 3178–3192. [CrossRef]
97. Breiman, L. Random forests. *Mach. Learn.* **2001**, *45*, 5–32. [CrossRef]
98. Elith, J.; Leathwick, J.R.; Hastie, T. A working guide to boosted regression trees. *J. Anim. Ecol.* **2008**, *77*, 802–813. [CrossRef] [PubMed]
99. Krause, P.; Boyle, D.; Bäse, F. Comparison of different efficiency criteria for hydrological model assessment. *Adv. Geosci.* **2005**, *5*, 89–97. [CrossRef]
100. Nash, J.; Sutcliffe, J.V. River flow forecasting through conceptual models part I—A discussion of principles. *J. Hydrol.* **1970**, *10*, 282–290. [CrossRef]
101. Janssen, P.; Heuberger, P. Calibration of process-oriented models. *Ecol. Model.* **1995**, *83*, 55–66. [CrossRef]
102. Harmer, R.; Kiewitt, A.; Morgan, G. Effects of overstorey retention on ash regeneration and bramble growth during conversion of a pine plantation to native broadleaved woodland. *Eur. J. For. Res.* **2012**, *131*, 1833–1843. [CrossRef]